CONCEPTUAL DESIGN OF THE D-^{3}He REACTOR ARTEMIS

D-^{3}He/FUSION REACTORS

KEYWORDS: *D-^{3}He fuels, field-reversed configuration reactor, conceptual reactor design*

HIROMU MOMOTA *National Institute for Fusion Science Nagoya 464-01, Japan*

AKIO ISHIDA *Niigata University, Niigata 950-21, Japan*

YASUJI KOHZAKI *Institute for Future Technology Tokyo 102, Japan*

GEORGE H. MILEY *University of Illinois Urbana, Illinois 61801*

SHOICHI OHI *Osaka University, Suita 565, Japan*

MASAMI OHNISHI *Kyoto University, Uji 611, Japan*

KUNIHIRO SATO *Himeji Institute of Technology Himeji 671-22, Japan*

LOREN C. STEINHAUER *STI Optronics, Inc. Bellevue, Washington 98004*

YUKIHIRO TOMITA *National Institute for Fusion Science Nagoya 464-01, Japan*

MICHEL TUSZEWSKI *Los Alamos National Laboratory Los Alamos, New Mexico 87545*

Received May 10, 1991
Accepted for Publication September 20, 1991

A comprehensive design study of the D-^{3}He-fueled field-reversed configuration (FRC) reactor Artemis is carried out for the purpose of proving its attractive characteristics and clarifying the critical issues for a commercial fusion reactor. The FRC burning plasma is stabilized and sustained in a steady equilibrium by means of preferential trapping of D-^{3}He fusion-produced energetic protons. A novel direct energy converter for 15-MeV protons is also presented. On the bases of consistent fusion plasma production and simple engineering, a compact and simple reactor concept is presented.

The D-^{3}He FRC power plant offers a most attractive prospect for energy development. It is environmentally acceptable in terms of radioactivity and fuel resources, and the estimated cost of electricity is low compared with a light water reactor. Critical physics and engineering issues in the development of the D-^{3}He FRC reactor are clarified.

I. INTRODUCTION

Progress in fusion research has been achieved mainly on tokamak experiments, and a scientific feasibility experiment will soon be performed on this concept. Nevertheless, a number of engineering problems have to be resolved before deuterium-tritium (D-T)–fueled tokamaks become acceptable commercial power reactors. Development of a reasonable tritium breeding blanket is one such problem.

Certain engineering problems for a commercial D-T fusion reactor are attributed to 14-MeV neutrons, and they seem to be very difficult to resolve. The 14-MeV neutrons damage the structural materials of the blanket. Embrittlement of these materials shortens their lifetime, which has been estimated[1,2] from the allowed maximum neutron fluence to be <10 MW·yr/m^2. It is preferred, therefore, to develop materials that retain their characteristics in a 14-MeV neutron environment for as long as 100 MW·yr/m^2. Disposal of a large amount of radioactive waste is an environmental problem because it takes more than several tens of years before the induced radioactivity decays to an inappreciable level.

Furthermore, a reasonable cost of electricity (COE) and high plant efficiency are required of a commercial power plant. In a conventional D-T fusion concept, 80% of the fusion energy is carried by 14-MeV neutrons to the blanket, then the heat energy is converted into electricity through turbines and generators. The overall plant efficiency is therefore limited by the efficiency of the turbine-generators.

Deuterium-^{3}He fusion fuels are considered to mitigate the engineering problems associated with 14-MeV neutrons. With those fuels, the fraction of 14-MeV neutrons in the total fusion power decreases to a few percent,[3,4] and >70% of the fusion power is carried by 14.7-MeV fusion protons and the diffused thermal fuel component. If these charged particles can be conducted[3] to direct energy converters, we can achieve a highly efficient fusion plant by employing D-^{3}He fuels. The confinement parameter $n\tau$ and the operation temperature T needed to sustain D-^{3}He fusion reactions are as high as 10^{21} s/m^3 and ~100 keV, respectively. To reduce the synchrotron radiation loss and consequently to obtain a higher plant efficiency, a large plasma beta value (>30%) is also recommended. High-power direct energy converters are needed to fully utilize the power carried by charged particles.

By its intrinsic characteristics, a field-reversed configuration (FRC) seems to meet the foregoing requirements. The plasma is confined by closed lines of force for good confinement and surrounded by open lines of force for extraction of charged particles. Since an FRC has no toroidal magnetic field for plasma stability, the stably confined FRC plasmas so far obtained in experiments[5,6] have had an extremely high beta value (>50%). Based on this, conceptual designs of D-^{3}He FRC fusion reactors have been carried out. The SAFFIRE is a very small, pulse-operated reactor concept[7] whose small size might be favorable for stability but is unfavorable for obtaining high plant efficiency. The RUBY is a 1-MW(electric) stationary-operated reactor concept,[8] which has many unresolved physics and engineering problems, especially in the area of plasma stability.

An FRC is experimentally stable against macroscopic tilt modes unless its s value (the ratio of plasma radius and averaged gyroradius of ions) is much larger than unity. If the s value is not large, a certain stabilization effect[9] is expected from the elongation of the FRC. Since the s value is proportional to the trapped magnetic flux Ψ as well as the separatrix radius, a representative s value for a few-gigawatt D-^{3}He FRC reactor is much larger than unity. Thus, one must employ a stabilizing method that will be effective in commercial fusion plants with a large s value. Stabilization by energetic charged-particle beams[10] in a large-s FRC has been demonstrated, analytically for rigid tilt modes[11] and numerically for full tilt modes.[12] One possibility for supplying the beam is the injection of energetic neutral particles. In a D-^{3}He burning plasma, however, the preferential trapping of fusion protons serves as an energetic particle beam that stabilizes tilt modes and also provides a major part of the seed current needed to sustain an FRC plasma in a steady burning equilibrium.

A conceptual design study of the D-^{3}He FRC fusion reactor Artemis has been carried out for the purpose of examining its attractive characteristics and clarifying critical issues for commercial fusion reactors. The design retains the essential features of RUBY but modifies them so as to describe a complete plasma scenario by making use of the stabilization effects due to energetic beam particles.

A significantly different D-^{3}He–fueled fusion reactor, Apollo (Ref. 13), has been studied based on a low-beta tokamak. In that design, >90% of the fusion energy is carried by radiation, so highly efficient rectifying antennas are needed. It appears that the D-^{3}He fuel enables the reactor to be inherently safe and the first wall to be permanent during the life of the reactor.

An overview of the Artemis reactor design is presented in Sec. II. Parametric studies on D-^{3}He fusion plasma are described, and the principal parameters of a steady equilibrium in a burning plasma are fixed in Sec. III. In Sec. IV, the startup of the FRC plasma to the D-^{3}He burning state is discussed. This is achieved by a compression of the external magnetic field, fuel injection, and neutral beam injection (NBI) of energetic particles. One of the key technologies of the Artemis design is direct energy conversion. We introduce a novel traveling wave direct energy converter in Sec. V. In Sec. VI, we verify the attractive characteristics of the Artemis reactor by estimating the COE; we find that the reactor is economical compared with a light water reactor (LWR). Finally, Sec. VII is devoted to discussions of the results and to critical issues for further studies.

II. OVERVIEW OF THE ARTEMIS REACTOR CONCEPT

The D-^{3}He–fueled FRC fusion reactor Artemis consists of a formation chamber, a burning chamber, and a pair of direct energy converters, all of which are

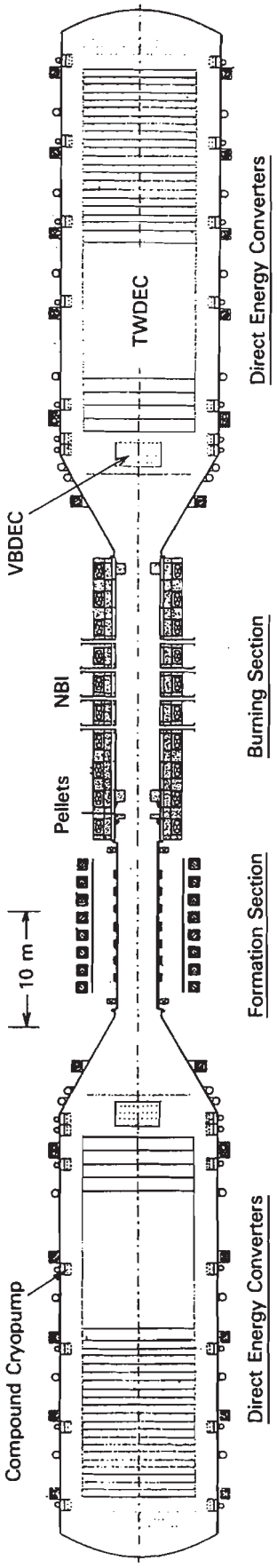

Fig. 1. The D-^{3}He FRC reactor Artemis, composed of a formation chamber, a burning chamber, and direct energy converters.

connected by magnetic lines of force (Fig. 1). An FRC plasma is produced at the start by the conventional reverse-biased fast theta-pinch method in the formation chamber and then translated to the burning chamber. A combination of deuterium NBI, fueling, and a slow magnetic compression in the burning chamber brings the volume, the temperature, and the number density of the plasma up to those for the D-^{3}He burning state. Most of the D-^{3}He fusion energy is carried by charged particles along the lines of force, which connect to a pair of direct energy converters. A smaller fraction of the fusion energy is carried by neutrons and photons to the first wall of the burning chamber. This energy is converted to electricity by turbine-generators.

II.A. Fusion Plasma

The formation chamber is arranged symmetrically so as to reduce error fields as much as possible. Therefore, only a small port for gas puffing is installed in the symmetrical coils and vacuum chamber system. Thus, reliable FRC plasma formations can be achieved even for a very low feed gas pressure. A fast-rising theta-pinch discharge with a one-turn voltage of 400 kV in a filling gas pressure of 0.05 Pa and bias field of 0.035 T produces an initial FRC plasma whose parameters are listed in Table Ia. The plasma is then translated to the burning chamber because of an unbalanced cusp magnetic field. During the translation, the FRC seems to conserve particle numbers of respective species, the total energy, the trapped flux, and its "intelligence." Plasma parameters obtained in this way at the burning chamber are listed in Table Ib.

In the burning chamber, the FRC plasma is heated by means of energetic deuterium NBI with a maximum power of 100 MW. A slow magnetic compression is also applied. The injected particles form an ion beam

TABLE I

Plasma Parameters

	Phase		
	a	b	c
Plasma radius (m)	0.7	1.0	1.12
Plasma length (m)	4.8	14.8	17.0
Plasma temperture (keV)	1.0	1.0	87.5
Electron density ($\times 10^{20}$/m^3)	4.1	0.62	6.6
Trapped flux (Wb)	0.086	0.086	3.66
External magnetic field (T)	0.56	0.22	6.7
s value	5.9	2.7	9.2
Plasma beta value	0.92	0.83	0.90

[a]After formation of the FRC.
[b]After translation of the FRC.
[c]Steady burning state.

current that serves as the seed current needed to sustain or increase the trapped magnetic flux of an FRC. The plasma evolves in its volume, the density, and the temperature for a burning plasma. During the evolution, the ratio of the current carried by the energetic beam particles to the total plasma current is high enough to stabilize an FRC against macroscopic modes. The set of plasma parameters obtained in this way is tabulated in Table Ic.

In a D-^{3}He burning FRC plasma, the current drive due to the preferential trapping of fusion protons assisted by a small amount of external beam injection is sufficient to sustain an equilibrium in a steady burning state.[14] The particle flows in this steady burning D-^{3}He FRC plasma are exhibited in Fig. 2, where the unknown particle transport is tentatively assumed to be 206 times the classical rate.[15]

II.B. Key Technologies

A fairly low feed gas pressure (0.05 Pa) and a high one-turn voltage of the pinch coils are needed to obtain an FRC with a low s value. Insulation for this high voltage is achieved by the four-stage tandem structure of the pinch coils.

Superconducting pulse coils of 1.87 (MA·turn)/coil at the formation chamber raise the magnetic field to 1.26 T in 50 ms. Fast coils for this compression (25 T/s, maximum of 1.26 T) are available with present technology; a fast-rising superconducting coil that gives a rise rate of 200 T/s and a maximum field of 4 T with a three-stage strand cable has been examined.[16] A large radius, 5 m, is chosen for the compression coils in order to reduce the coupling with the 2.1-m-radius coaxial pinch coils, with the assistance of magnetic shielding plates.

Pellet acceleration is one of the most important engineering problems in fusion research: A representative speed needed to inject a pellet deeply into a plasma center is several times 10^4 m/s, which may be compared with the currently available speed of 10^3 m/s. In the Artemis design, however, a 1.8-mm^3 pellet consisting of an iced cylindrical deuterium vessel and inner liquid ^{3}He is dropped every 0.9 s. Fabrication of the pellet is rather simple. When a pellet is located near the center of the chamber, the FRC plasma moves toward the pellet at a high speed ($>10^4$ m/s) with the aid of an applied cusp field and consequently engulfs it deeply inside the plasma.

A set of ten superconducting coils of 14.2 (MA·turn)/coil and 3.5-m radius is installed at the burning chamber and supplies a magnetic field of 6.7 T. The required average current density of 30 A/mm^2 is conventional, and the 300-MPa stress is easily held by the reinforced structure of the strand cable.

To heat the plasma as well as drive the plasma current that is needed to sustain the plasma in a steady equilibrium, injection of 1-MeV deuterium neutral beam particles is employed. A maximum power of 100 MW is required for startup and 5 MW to sustain the plasma in the steady burning state. The development of this neutral beam is within the scope of research and development programs for the International Thermonuclear Experimental Reactor (ITER).

One of the most important technologies to be developed for a D-^{3}He FRC reactor is the direct conversion of the fusion power carried by charged particles. For the thermal component of a plasma, a "venetian-blind-type" generator[17] (VBDEC) might be applicable. For 14.7-MeV fusion protons, however, the energy is too high to maintain the necessary electrical insulation. The concept of a traveling wave direct energy converter[18] (TWDEC) is developed based on the principle of a linac.[19]

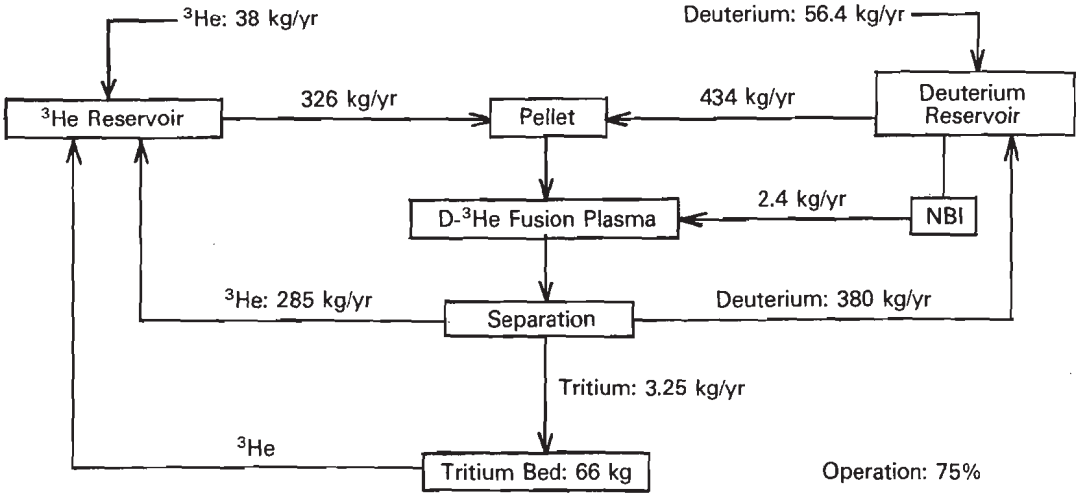

Fig. 2. A chart of particle flows in Artemis. Some of the fusion particles are lost directly, and others are diffused out of the plasma.

TABLE II

Principal Parameters of the D-^{3}He FRC Fusion Reactor Artemis

Fusion power (MW)	1610
Charged particles	1181
Neutron	77
Radiation	357
Electric power (MW)	1052
Through direct energy converters	808
Through turbine-motor generators	244
Fusion plasma	
Volume (m^3)	67 ($r_s = 1.12$ m, $l_s = 17$ m)
Fuel	D-^{3}He, $n_{^3He}/n_d = 1/2$
Average electron density (m^{-3})	6.6×10^{20}
Temperature, $T_i = T_e$ (keV)	87.5
Beta value (%)	90
Chamber	
Formation chamber	$r = 1.8$ m, $L = 15$ m, $t = 0.15$ m, alumina tubes
Burning chamber	$r = 2.0$ m, $L = 25$ m, $t = 0.05$ m, ferritic steel
Heat load on the first wall (MW/m^2)	1.70
14-MeV neutron load on the first wall (MW/m^2)	0.27
Energy conversion chamber	$r = 10$ m, $L = 50$ m, stainless steel vessel
Magnetic coils	
Pinch coils	$r = 2$ m, $L = 10$ m, five-stage tandem, copper, $L_c = 1.6$ μH
Pulse coils	$r = 5$ m, NbTi/Cu/CuNi, maximum 200 T/s, 4 T, 1.87 (MA·turn)/coil, 8 coils
Slow coils	$r = 3$ m, NbTi/Cu/CuNi, maximum 7 T, 14.2 (MA·turn)/coil, 10 coils
Heating and current drive	NBI
Startup	Maximum 1400 keV, 100 MW, D^0 injection
Steady burning	1000 keV, 5 MW, D^0 injection
Fueling	Packman method, liquid ^{3}He in an iced deuterium vessel
Deuterium (kg/yr)	56.4
^{3}He (kg/yr)	38.0

II.C. Reactor System

A conceptual design for the D-^{3}He FRC power reactor Artemis has been carried out; the power flowchart is shown in Fig. 3. All of the technological bases employed for this design are conventional. The efficiency of the conversion from heat energy to electricity is assumed to be 36%. Owing to the high efficiency of the direct energy converters, the overall plant efficiency is estimated to be as high as 62%. The principal parameters of the plant are shown in Table II. The device consists of straight tubes forming a linear geometry; thus, it is easy to disassemble for maintenance.

On the basis of a study[20] by the Senior Committee on Environmental, Safety, and Economic Aspects of Magnetic Fusion Energy (ESECOM), the COE has been estimated for the Artemis design, as summarized in Table III. An average load factor of 75% is assumed. Note that the fuel cost (cost of ^{3}He obtained from the lunar soil[21] assumed to be \$200 000/kg) contributes only 4%. Since the total weight of the reactor, excluding the NBI, is ~3300 t, which is one-third that of a corresponding LWR, and the geometry is very simple, the estimated COE is as low as 28.7 mill/kW·h in Artemis, which is lower than the estimated COE

TABLE III

Cost of Electricity from the Artemis Design

(millions of dollars per year)

Capital cost	146.0	0.0844 × 99
Operation and maintenance	34.6	0.020 × 99
Fuel cost	8.0	40 kg/yr at \$200 000/kg
Total cost	188.6	
Cost of electricity (average load factor of 75%)		28.7 mill/kW·h

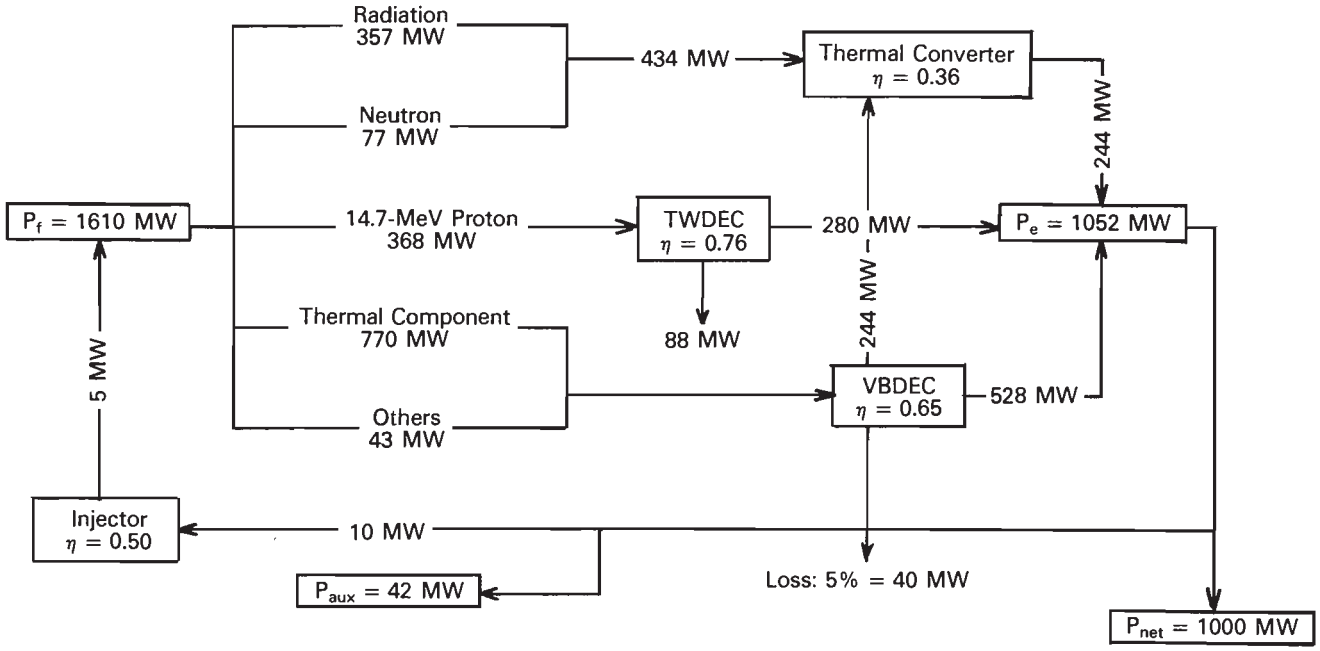

Fig. 3. Power flow diagram of Artemis. On the basis of highly efficient direct energy converters, the overall plant efficiency is as high as 62%.

from a present-day LWR [33.4 to 56.6 mill/kW·h (Ref. 22)].

III. D-^{3}He FUSION PLASMA

The favorable characteristics of D-^{3}He fusion fuels result from the small amount of 14-MeV neutrons and higher radiation parameter (the ratio of the power introducible to direct energy converters to the total fusion power). On the other hand, the required ignition product $n_e\tau_E T$ is 25 times larger than that of D-T fuels. The 14-MeV neutron power fraction (the ratio of the power carried by 14-MeV neutrons to the total fusion power), the radiation parameter, and the $n_e\tau_E T$ for ignition are shown in Fig. 4 against the concentration of ^{3}He and deuterium, where a plasma temperature of 90 keV and an average beta value of 90% are assumed. The ratio of the particle confinement time and the energy confinement time is assumed to be 2. The radiation loss increases through an increase in the effective Z, and the 14-MeV neutron fraction decreases as the fuel ratio increases. On the basis of these

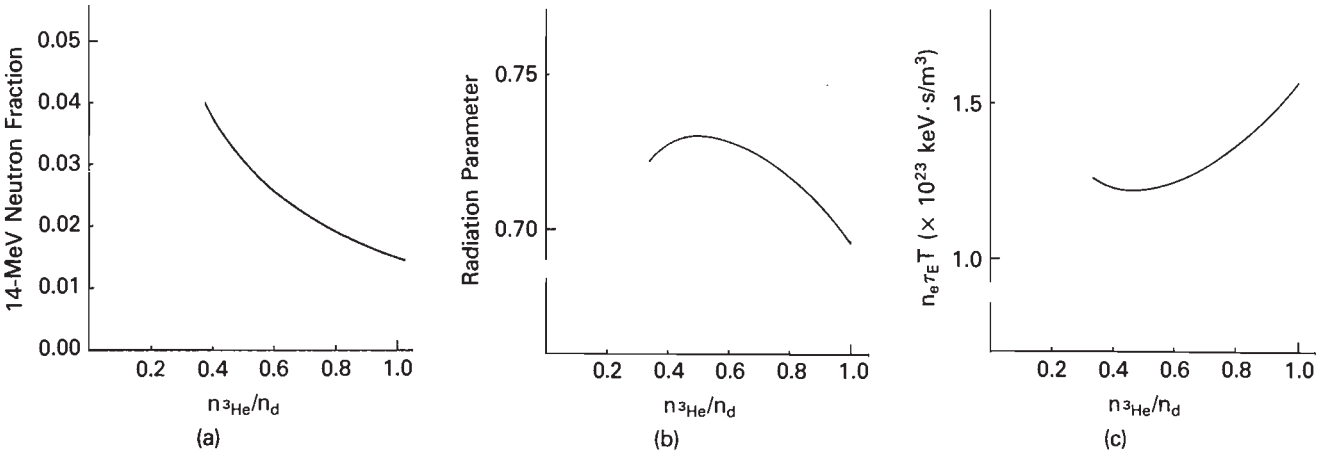

Fig. 4. (a) The 14-MeV neutron power fraction, (b) radiation parameter, and (c) triple product $n_e\tau_E T$ versus the concentration of ^{3}He and deuterium. A plasma temperature of 90 keV and an average beta value of 90% are assumed. The ratio of the particle confinement time and the energy confinement time is assumed to be 2.

calculations, we employ a deuterium-to-^{3}He density ratio of 1/2, which maximizes the radiation parameter and minimizes the required ignition product.

Characteristics such as the 14-MeV neutron fraction, the radiation parameter, which is approximated by the ratio of power conducted to direct energy converters and fusion power, and the confinement parameter $n_e\tau_E$ for ignition of D-^{3}He fusion plasma change as the operation temperature changes. Figure 5 shows respective values versus the operating temperature. The average beta value is still assumed to be 90%. The particle confinement time is assumed to be twice the energy confinement time. As can be seen in Figs. 4 and 5, a D-^{3}He plasma temperature of 70 to 100 keV and a ^{3}He density of 0.4 to 1 times the deuterium density are recommended to obtain a favorable fusion plasma. We choose a plasma with a temperature of 87.5 keV and a ^{3}He density of one-half the deuterium density. Note that elastic scattering of energetic particles is ignored in these calculations. It is expected that the 14-MeV neutron fraction and the required ignition product will decrease and the obtained radiation parameter will increase once elastic scattering is taken into account, because it increases the high-energy tail of the distribution function of the fuel components and consequently enhances the D-^{3}He reaction.

In a D-^{3}He burning FRC plasma, the momentum transfer from a directed flow of fusion particles causes a rotation of the background fuel plasma around the axis of symmetry. Consequently, the conventional analysis for obtaining an equilibrium by solving the Grad-Shafranov equation is no longer applicable. We developed, therefore, a reasonable method[23] to obtain the steady-state equilibrium of a burning FRC plasma: We solve a set of equations for the respective species of the fuel plasma describing the static balance between inputs and losses in terms of particle numbers, momenta, and energies. The equilibrium is then obtained in terms of the input of particles, momentum, and energy. A solution at the midplane obtained for this design is shown in Fig. 6. A uniform distribution of the plasma temperature, as is normally observed in experiments, is assumed. Microscopic turbulence was also introduced so as to cause an anomalous transport factor of 206. The total current for an FRC is estimated to be 160 MA for a 1.12-m separatrix radius and a 17-m plasma length. A seed current of 50 MA is needed to sustain the plasma in the steady-state equilibrium. Since the plasma temperature is very high and, consequently, the slowing down of an energetic particle is very small, the 50-MA seed current is obtained by steadily injecting 1-MeV beam particles with an effective current of 22 A. Fortunately, an appreciable amount of this seed current (42 MA) is naturally supplied in D-^{3}He burning FRC plasma by the proton beam arising from the preferential trapping of 14.7-MeV fusion protons. Consequently, the injection of 1-MeV beam particles with a current of <5 A is enough to sustain the plasma in the steady burning equilibrium.

A set of plasma parameters obtained in this manner is listed in Table IV. For an 87.5-keV plasma temperature, a ^{3}He-to-deuterium density ratio of 1:2, and an electron density of $6.6 \times 10^{20}/m^3$, the required energy confinement time τ_E is 2.1 s. Observe that 74% of the fusion power is carried by charged particles. The plasma volume and input power are as small as 67 m^3 and 5 MW, respectively. These characteristics result in a highly efficient power plant using D-^{3}He fuels in an FRC.

In the D-^{3}He burning FRC plasma, tilt modes may be stabilized by energetic beam particles as was demonstrated by Barnes and Milroy.[12] The beam current must exceed 20 to 25% of the total current for stabilization by this means. Further, rotational modes

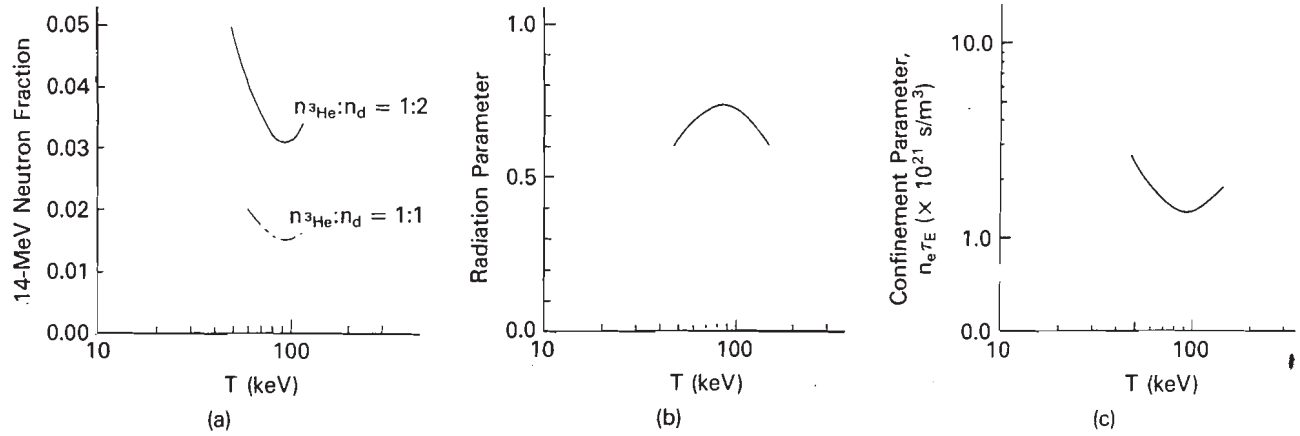

Fig. 5. (a) 14-MeV neutron fraction, (b) radiation parameter, and (c) confinement parameter $n_e\tau_E$ of a D-^{3}He fusion plasma versus the operation temperature. The average beta value is assumed to be 90%, and the ^{3}He density is chosen to be one-half of the deuterium density. The particle confinement time is assumed to be twice the energy confinement time.

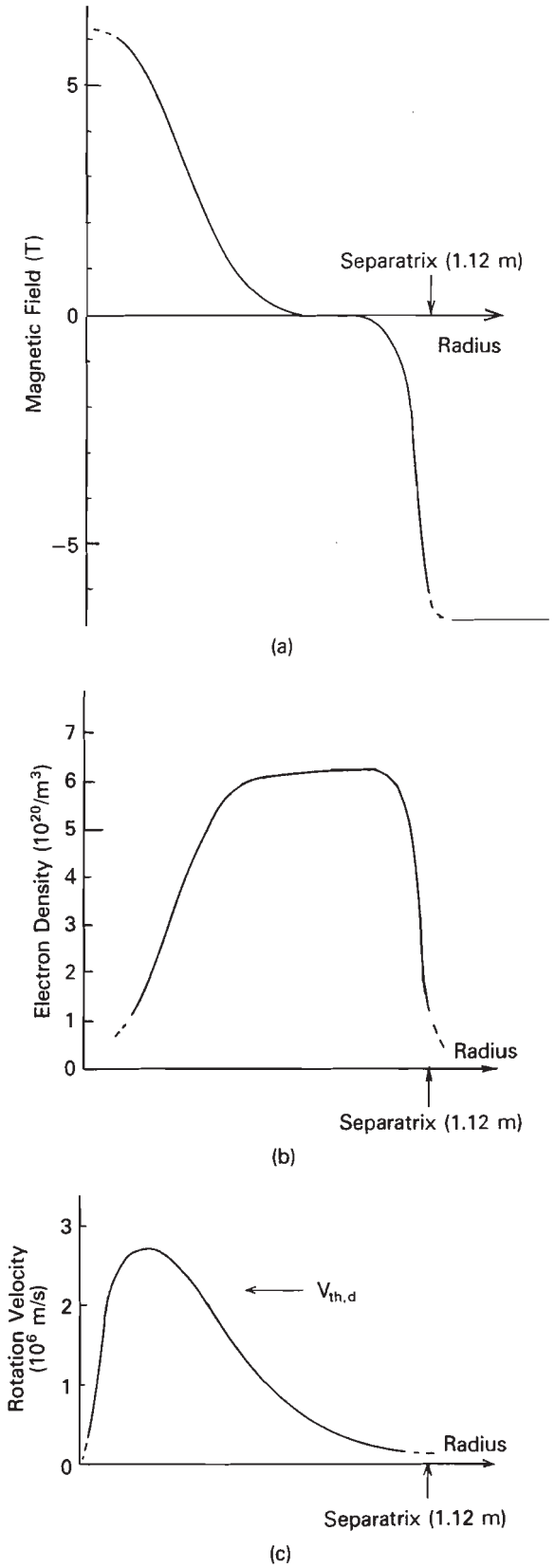

Fig. 6. A steady-state equilibrium at the midplane of the burning FRC plasma: (a) the magnetic field, (b) the electron density, and (c) the rotation velocity.

TABLE IV

Plasma Parameters of a Steady Burning D-^{3}He FRC

Fusion power (GW)	1.6
14.7-MeV protons (MW)	368
Neutrons (MW)	77
Thermal ions (MW)	770
Radiation (MW)	357
Other fusion products (MW)	43
Plasma	
Volume (m^3)	67.0
Radius (m)	1.12
Length (m)	17.0
Number density of electrons	6.6×10^{20}/m^3
Deuterium	2.9×10^{20}/m^3
^{3}He	1.4×10^{20}/m^3
Others	0.6×10^{20}/m^3
Fueling	7.8×10^{21}/s
Pellet injection	7.77×10^{21}/s
NBI	3.1×10^{19}/s
Plasma temperature (keV)	87.5
Current drive	1 MeV × 5 A (NBI)
Energy confinement time (s)	2.09
Particle confinement time (s)	4.18
External magnetic field (T)	6.7
Beta value	0.90

may also be stabilized[24] with the aid of a beam current of only a few percent of the total current. A particle beam current of 27.5% of the total current is regarded as sufficient to stabilize all macroscopic modes.

IV. STARTUP OF THE FUSION PLASMA

An FRC plasma is first formed at the formation chamber where a set of seven pinch coils, a set of eight fast coils, and two pairs of cusp coils are installed. A cross-sectional drawing of the formation section is shown in Fig. 7. Coaxial fast coils are magnetically shielded from the pinch coils so as to avoid an induced high voltage. Each pinch coil has a four-stage tandem structure that forms a series circuit with power sources, as is illustrated in Fig. 8. A bias field of −0.035 T together with the two cusp coils yields cusped magnetic field structures at both ends of the device. A fast-acting gas puff for feeding 52 mPa of mixed D_2 and ^{3}He gas and the low-voltage circuits of the pinch coils are activated at time $t = -1$ ms, then the high-voltage circuits are closed at time $t = 0$. At time $t = 5$ ms, the current in the fast superconducting coils starts to rise rapidly to supply the guide magnetic field that connects the burning chamber and the direct energy converter. Representative characteristics of the pinch coils and fast superconducting coils are listed in Table V, together with those of the slow superconducting coils at the burning

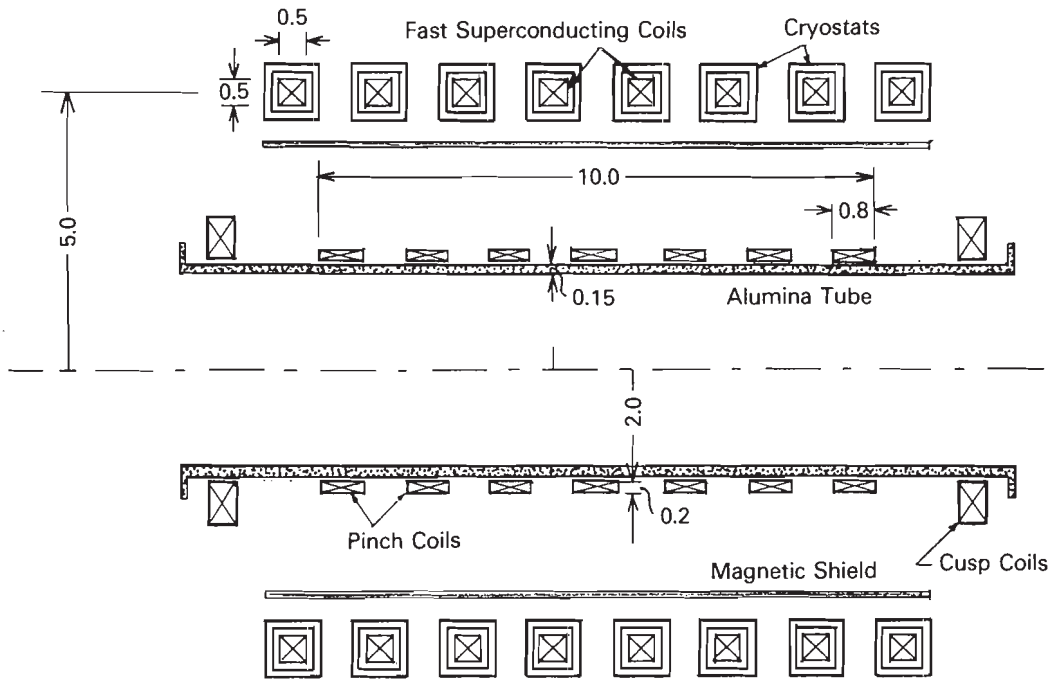

Fig. 7. A cross section of the formation chamber, which consists of a set of pinch coils for FRC formation, a set of fast coils for a guide field, and two cusp coils operated together with pinch coils.

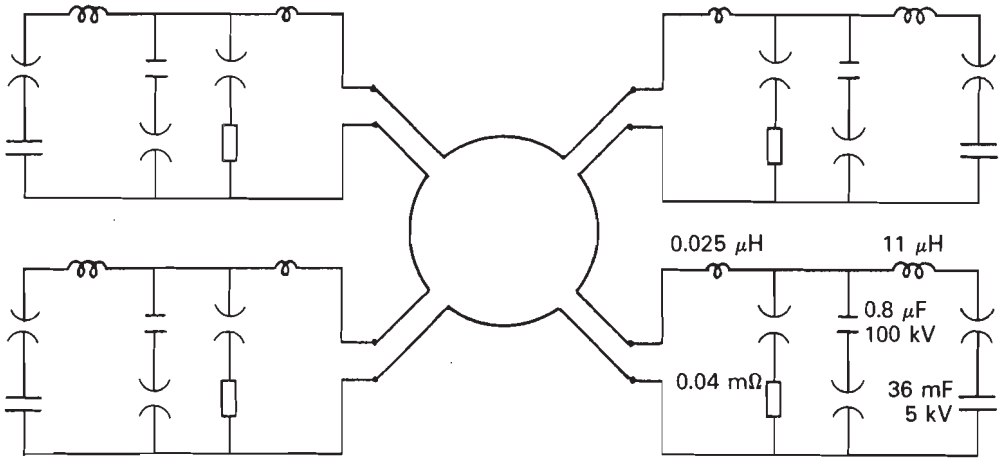

Fig. 8. The electric circuits for four-stage tandem pinch coils.

chamber. The gases are ionized and compressed until $t = 4.8\ \mu s$. The plasma expands for the following $0.7\ \mu s$, and the formation of an FRC plasma is completed. The plasma is then compressed adiabatically, as is seen in Fig. 9. The parameters of the FRC plasma are listed in Table Ia. After the formation of an FRC, the plasma is translated by applying the unbalanced cusps toward a magnetic bottle at the burning chamber.

The number of confined particles for the respective species, the total energy, and the trapped magnetic flux in the FRC are conserved during the translation because the duration of the translation is much shorter than the characteristic time of dissipation. This condition determines the plasma parameters just after the translation, as is exhibited in Table Ib.

In the burning chamber, the FRC plasma is heated by means of injected energetic beam particles whose maximum total power is limited to 100 MW, which also provides the seed current and consequently sustains or enhances the trapped flux of the FRC. D-^{3}He pellets are also injected to resupply the fuel, and the applied external magnetic field is raised from 0.22 to

TABLE V

Characteristics of Magnetic Coils

	a	b	c
Inner radius (m)	2.0	4.75	3.25
Outer radius (m)	2.2	5.25	3.75
Length of a coil (m)	0.8	0.5	1.0
Number of coils	7	8	10
Total length (m)	10	12	30
Cable	Copper	NbTi superconducting strand	NbTi superconducting monolith
Total current (MA·turn)	4	15	142
Maximum field (T)	0.56	4.0	7.1
Period	10 μs	20 T/s dc	dc

[a]Pinch coils for FRC formation.
[b]Fast coils for the guide field in the formation chamber.
[c]Slow coils for FRC confinement.

6.7 T for 50 s. A cross-sectional drawing of the burning section is given in Fig. 10, where eight NBI ports and one port for pellet injection are installed. The temporal values of the applied external magnetic field, the input NBI power, and the number of injected particles are shown in Fig. 11. Plasma parameters such as the plasma temperature T, the plasma radius r_s, and the plasma length l_s develop in accordance with the continuity of the particle species, the energy conservation, and the force balance. Since the transport coefficients relevant to burning plasma in an FRC are unknown, particle transport with a temperature-dependent anomalous multiplier of $10 + 0.244 \times (T/\text{keV} - 1)^{3/2}$ to the classical particle transport and an energy transport of twice the particle transport are tentatively assumed. The consequent development of the plasma is shown in Fig. 12. At time $t = 50$ s, the plasma parameters reach the values required for D-^{3}He burning. Since the ratio of the current carried by energetic particles to the total current exceeds 0.25 during the development, the FRC plasma should be stable. In this way, we have a burning FRC plasma with representative parameters as listed in Table IV.

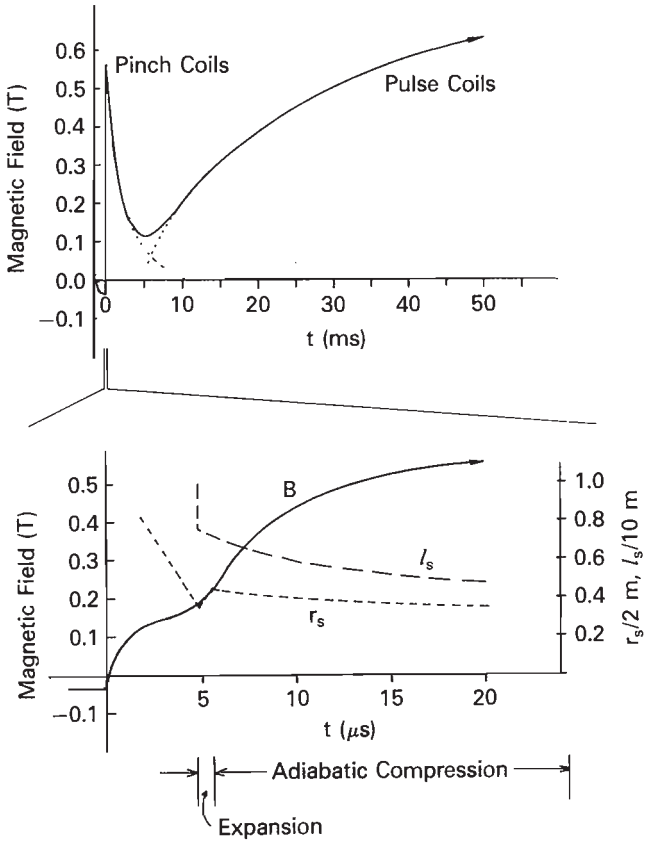

Fig. 9. The time sequence of applied external magnetic fields, the separatrix radius r_s, and the length l_s of the obtained FRC.

V. DIRECT ENERGY CONVERSION

Since a large amount of fusion power is carried by charged particles in a D-^{3}He burning FRC reactor, the use of highly efficient direct conversion of the energy into electricity is recommended to achieve an attractive fusion power plant. The application of direct energy converters in a plasma device is often a serious problem because a fairly large area of ion collector plate may be required to decrease the input power density and for heat removal. Fortunately, an FRC plasma is surrounded by open lines of force and is thus suitable for the application of direct energy converters.

The fusion power carried by charged particles consists of 810 MW of thermal ions and 368 MW of 14.7-MeV protons in the Artemis design. The energy spectrum of the former includes a thermal spread of

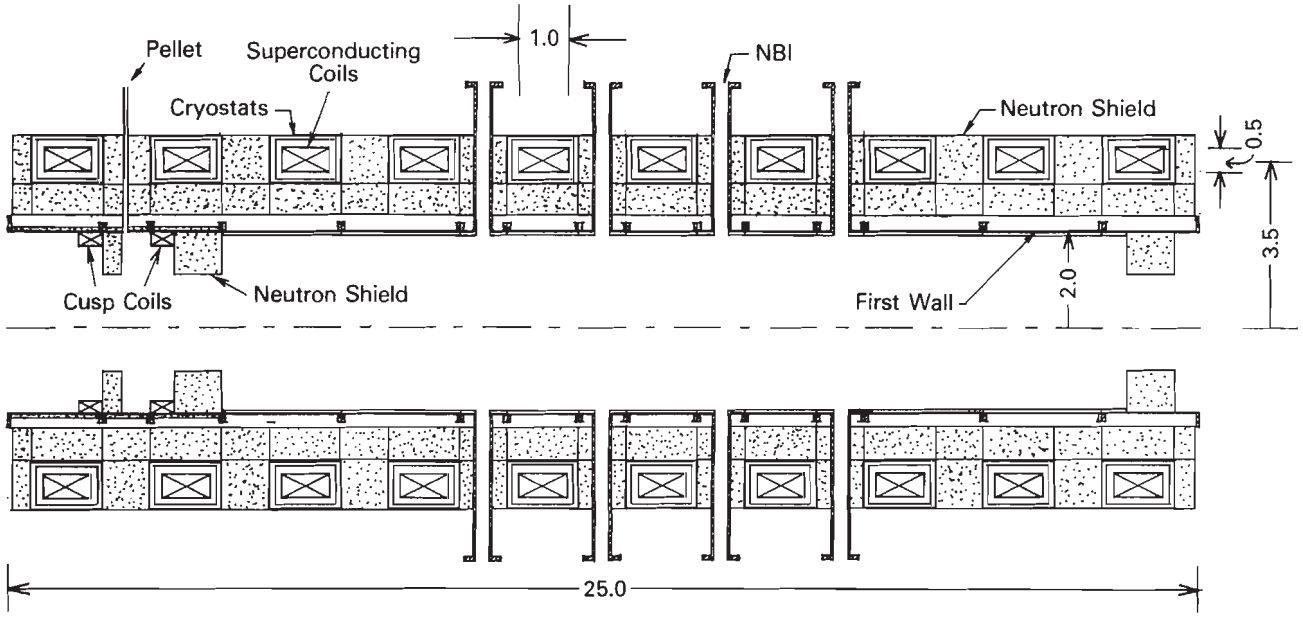

Fig. 10. A cross-sectional drawing of the burning section.

420 keV with a biased energy of $Z_j e\phi$, where Z_j is the charge number of the ions specified by subscript j, and $\phi = 135$ kV is the ambipolar potential attributed to a prompt loss of electrons along the lines of force. Note that these values are consistent with our assumptions, i.e., $\tau_n/\tau_E = 2$. Recalling[25] that the flashover voltage V (in kilovolts) is between $35 \times g^{0.5}$ and $35 \times g^{0.6}$ in a hydrogen atmosphere of <0.1 Pa, where g is the gap length (in millimetres), one is able to decelerate most of the thermal ions with the use of a direct current voltage and a reasonable gap length. In our design, VBDECs with five-stage fin arrays are employed, based on the RUBY design,[8] to obtain a higher conversion efficiency. Examples of ion orbits in the direct energy converter are exhibited in Fig. 13; and the size and the applied voltage of the ion collector for respective stages are listed in Table VI. The 2-m radius and 2.2-m length of the assembly are enough to recover the energy of the thermal component with an efficiency of 60%.

A pair of TWDECs are installed at both downstream ends of the VBDECs. These are designed to convert the kinetic energy of 14.7-MeV protons whose energy is too high to control by an electrostatic potential. Each converter consists of two parts. One part is the modulator, which modulates the velocity of the 14.7-MeV proton beam by an electrostatic propagating sawtooth wave whose wavelength is λ_0, and the applied maximum potential is V_m. The phase velocity of this wave is chosen to be the same as the velocity V of 14.7-MeV protons, i.e., 5.3×10^7 m/s. Then the proton beam is modulated and focused at $x_f = (\lambda/4) \times (14.7\ \text{MeV/eV}_m)$ measured from the downstream side of the entrance of the modulator. The other part of the converter is a decelerator in which a set of mesh grids

TABLE VI

Applied Voltage and Size of the Ion Collectors

	Stage				
	1	2	3	4	5
Separation between fin array (m)	0.34	0.32	0.39	0.52	0.79
Length of ion collector (m)	0.66	0.62	0.61	0.62	1.0
Applied voltage (kV)	132	245	394	607	954
Obtained electricity (MW)	45.8	53.8	51.9	39.8	28.6

Distance between ion collector plates (m)	0.25
Thickness of ion collector plate (m)	0.012
Angle between arrays and lines of force (radian)	0.044
Total length of the assembly (m)	2.2
Radius of the assembly (m)	2
Efficiency of the converter (%)	60.8

with an entrance at $x = x_f$ provides a traveling electrostatic wave

$$V(x,t) = V_d \cos\left[\int_x k(\xi)\, d\xi - \omega t\right] .$$

The bunched 14.7-MeV protons are trapped in phase ϕ of the wave, provided that the phase velocity of the wave is close to the velocity (5.3×10^7 m/s) at the entrance. The phase velocity of the applied traveling wave decreases with decreasing gap distance between the grids in the direction of the beam so as to lower the energy of the protons to a range suitable for VBDECs.

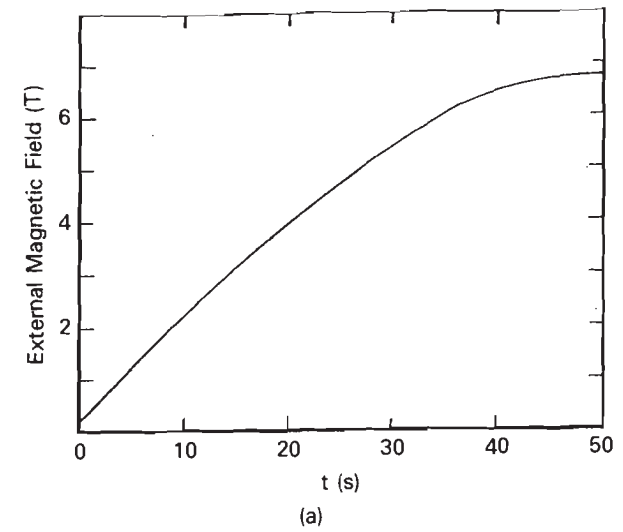

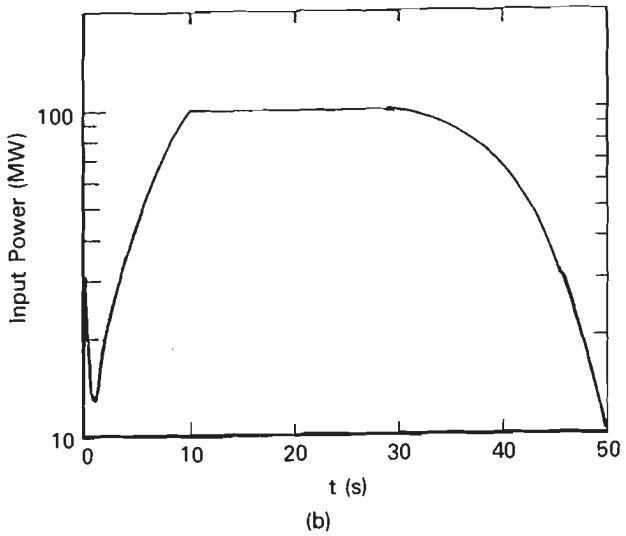

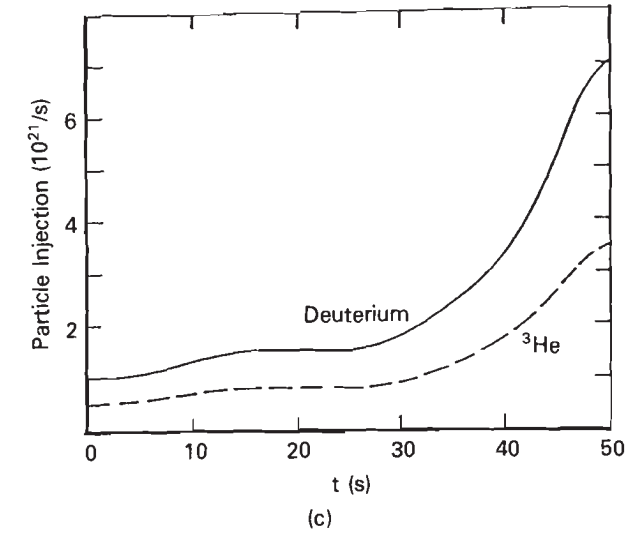

Fig. 11. (a) The applied external magnetic field, (b) the input NBI power, and (c) the number of injected particles with pellet per second.

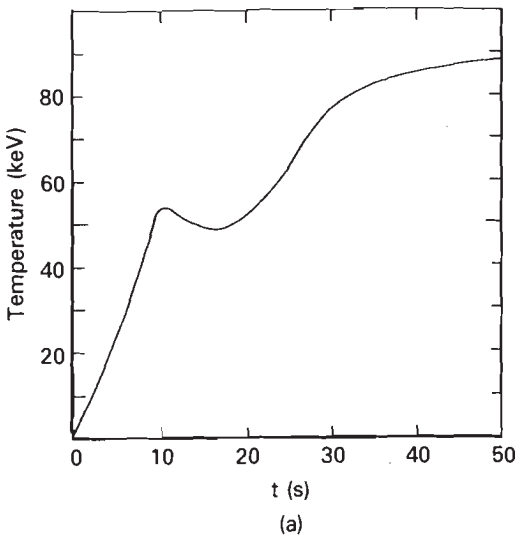

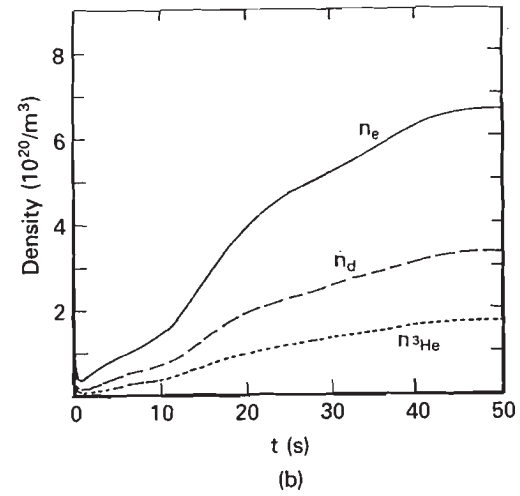

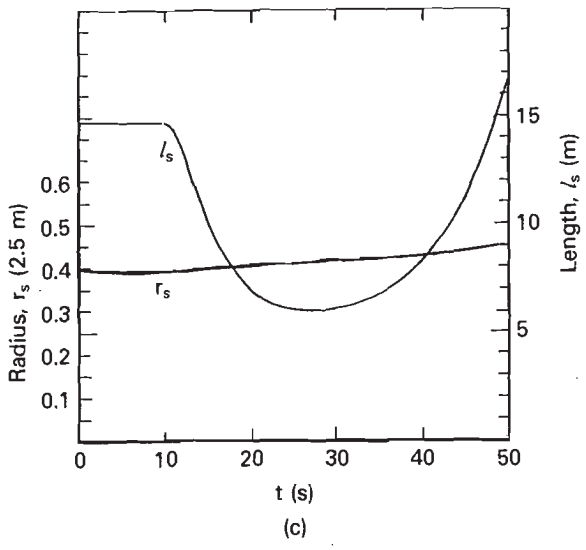

Fig. 12. A development of plasma attributed to the injection (Fig. 11): (a) temperature, (b) average density, and (c) radius and length.

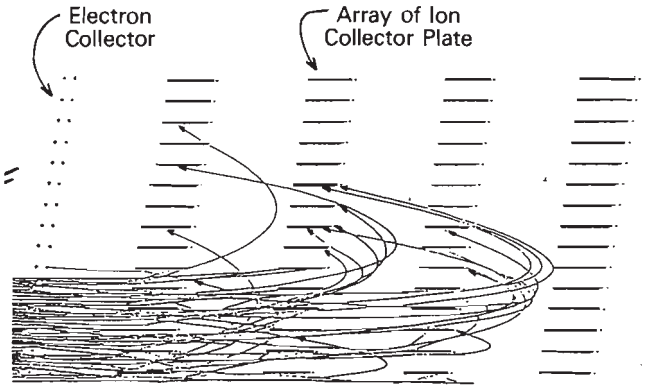

Fig. 13. Examples of orbits of thermal ^{3}He ions at the VBDEC.

The focus of the proton beam is spread, however, because of a thermal spread of fusion protons, which is analogous to that due to the spreading of the wavelength of a light beam. The spreading of the focus spoils the trapping of the protons within the traveling wave and eventually lowers the efficiency of the TWDEC. To examine the trapping and deceleration of the fusion protons, particle trajectory calculations were carried out, one of which can be seen in the phase-space plots of Fig. 14. A 4.7-m wavelength was employed for the modulator and the entrance of the decelerator. By applying the maximum voltage V_m of 0.82 MV to the modulator, the fusion protons are bunched and then trapped around a phase $\phi = 5\pi/6$ behind the peak of the applied traveling wave potential, whose maximum voltage $V_d = 0.42$ MV. More than 95% of the 14.7-MeV beam protons are trapped during the deceleration; however, a certain fraction of protons once trapped will be lost through collisions with the mesh structure of the grids.

The assembly of the TWDEC consists of 24 mesh grids: 5 for the modulator and 19 for the decelerator, located as shown in Fig. 15. Each mesh grid is made of 17-mm-diam × 1-mm-thick water-cooled pipes separated by 1.3 m. A pressure difference of 5 MPa is applied to cool the pipes, and the stress due to pressurized water is 40 MPa, which is much smaller than the allowable limit for this pipe. The total power needed to cool the grid is estimated to be 140 kW. The energy flow in the TWDEC of this structure is exhibited in Fig. 16. The total flux of 14.7-MeV protons is 183 MW or 7.8×10^{19}/s into the TWDEC. A power of 131 MW is extracted with a set of mesh grids, and a power of 12 MW is carried to the end collectors where 5.9 MW is collected as electricity. Thus, the total efficiency of the TWDEC for fusion protons is ~75%.

VI. EVALUATION OF THE D-^{3}He ARTEMIS DESIGN

We attempt to evaluate the Artemis reactor for the purpose of clarifying its favorable characteristics and indicating the optimum direction of the development. In estimating various energy systems or conceptual designs, it is important to compare these systems with a unified standard that allows a wide range of variations. Comparisons of this type have been made in the United States, and a frame of estimating the standard cost of fusion reactors, LWRs, advanced fission reactors, and various power plants has been devised. An assessment of the competitive potential of magnetic fusion energy compared with present and future fission energy sources has been completed by ESECOM.

The basis for calculating the COE of the Artemis reactor is to estimate the mass of components presented in the design and integrate them after multiplying the unit cost (dollars per kilogram), which is given

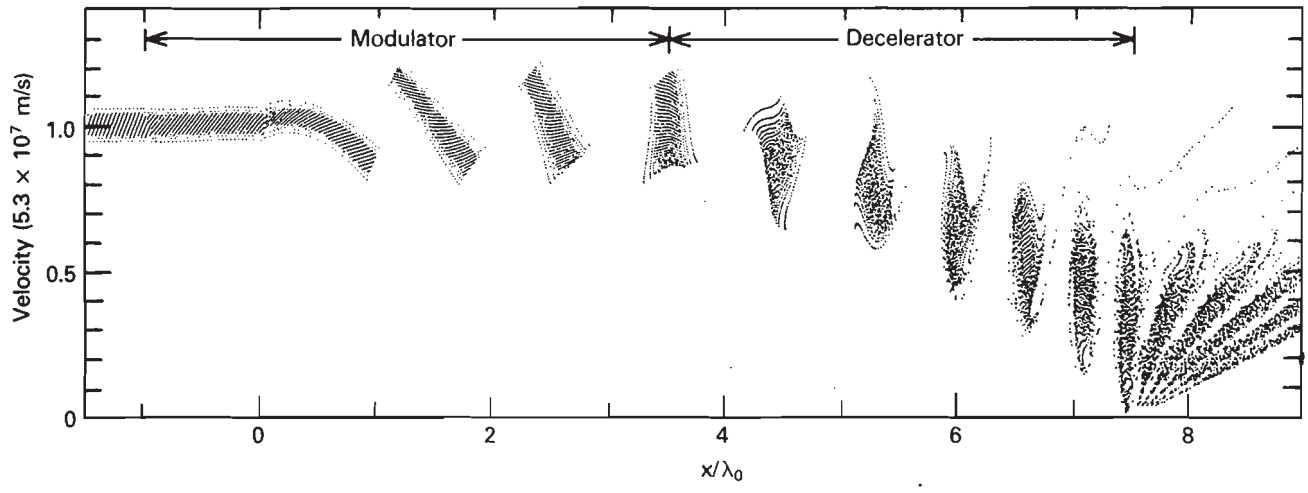

Fig. 14. Phase-space plots of fusion protons. The applied maximum voltage at the modulator and at the entrance of the decelerator are, respectively, 0.82 and 1.05 MV; 95% of the protons are trapped and decelerated.

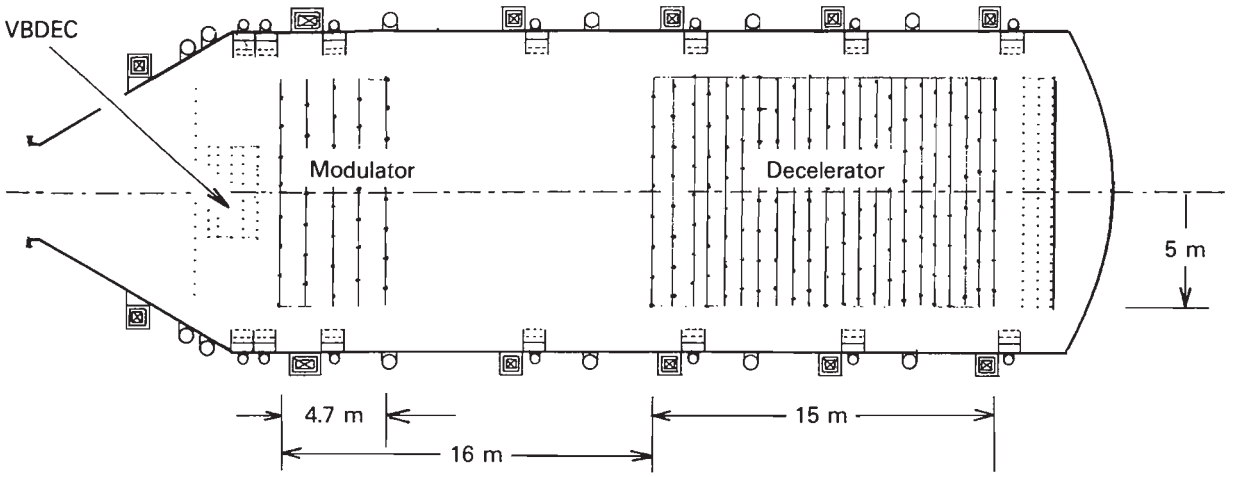

Fig. 15. Assembly of a TWDEC.

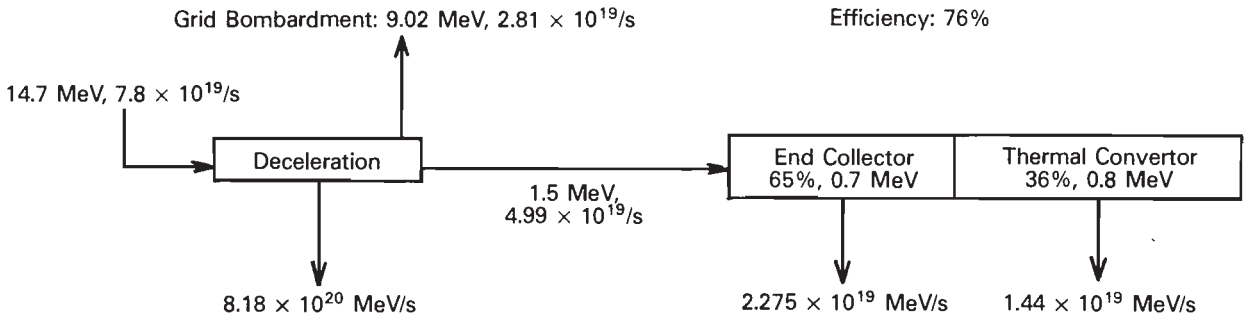

Fig. 16. An energy flowchart of the TWDEC.

by the ESECOM standard. For the cost of a component whose engineering base is the same as a conventional component, however, we introduced appropriate scaling rules. A summary of the total plant capital cost is presented in Table VII. The following assumptions have been made: Interest during construction is 0.0856, plant life is 30 yr, and the indirect cost factor is 0.581. The cost of fuel for the Artemis reactor is assumed to be \$200 000/kg, roughly twice that assumed in the ESECOM study. In Table VII, one finds that the total mass of the reactor is as small as 3300 t, which is one-third the weight of the primary system of an equivalent LWR and one order of magnitude smaller than that for an equivalent D-T tokamak reactor design. This is because the FRC plasma is compact and the plant efficiency is as high as 62%. The small amount of the total mass results in a small total capital cost for the plant.

On the basis of these cost analyses, the COE is estimated (Table III) to be 28.7 mill/kW·h. The COE is compared with that from a D-T tokamak reactor design or from LWRs. The cost of ^{3}He, which we assumed to be obtainable from the lunar surface, is \$200 000/kg and accounts for only 4% of the COE. In case of increased fuel cost, e.g., \$1 million/kg, the increase in the COE is only 17%.

A confinement anomaly factor of 206 is assumed for the burning state of this design. For a larger anomaly factor, the size of the fusion plasma is increased so as to meet the requirement for the confinement parameter ($n_e\tau_E = 1.38 \times 10^{21}$ s/m^3). A limiting factor for the size may be the stress of the magnetic coils (<300 MPa for the Artemis design), which is much lower than the estimated limit of 800 MPa. Another factor that limits the reactor size may be the wall load of 14-MeV neutrons. The wall load of 0.27 MW/m^2 in the Artemis design enables the life of the first wall to exceed the life of the reactor, i.e., 30 yr. For an anomaly factor of 1000, the magnetic field should be changed by 5.3 T, and the size of the reactor should be larger by a factor of 2.8. Both the maximum stress of the coils (300 MPa) and the 14-MeV neutron load onto the first wall (0.27 MW/m^2) remain unchanged. The net output power changes, on the other hand, to several gigawatts. Thus, the technological flexibility of the D-^{3}He–fueled FRC reactor enables the design to meet large varieties of unknown parameters.

Another area where the Artemis power plant has

TABLE VII

Total Plant Cost*

Account Number	Description	Cost (millions of dollars)		Mass (t), Unit Cost, Scale	
20	Land	5.0			
21	Structures and site facilities	196.9			
212	Reactor building	132.2		3.0	$118.6 \times (V/2.5)^{0.67}$
213	Turbine building	14.8		244.0	$35.92 \times (Pt/1440)^{0.50}$
214	Reactor maintenance building	49.8		1000 MW(electric)	
22	Reactor plant equipment	520.4			
221	Reactor system	404.4			
2211	First wall and blanket		12.9		
	Formation chamber		3.2	106	Alumina \$30/kg
			0.3	10.6	Stainless steel \$25/kg
	Burning chamber		9.5	189	HT \$50/kg
2212	Shield		20.6	589	Stainless steel + B_4C \$35/kg
2213	Magnet system		56.4	3.0	$118.6 \times (V/2.5)^{0.67}$
	Superconducting magnet		55.0		
			(33.0)	1000	NbTi/Cu \$33.3/kg
			(2.1)	60	Stainless steel can \$34.6/kg
			(19.9)	600	Stainless steel support \$33.2/kg
	Pinch coil		1.4	100	Copper \$14/kg
2214	Heating system (NBI)		225.0	100 MW	NBI \$2.25/W
2215	Structure		8.0		
2216	Vacuum vessel pumping system		4.0		
2217	Power plant and capacitor banks		15.5	33 MW	\$0.47M/MJ
2218	Direct energy converter		62.0		
			0.2	3.1	Grid \$50/kg
			12.0	600	Chamber \$20/kg
			49.8	808 MW	Electric equipment
222	Main cooling system	28.4		678 MW	$93.1 \times (P_{th}/4000)^{0.67}$
223	Auxiliary cooling system	10.8		1610 MW	$19.8 \times (P_f/4000)^{0.67}$
224	Radioactive waste facility	0.5		77 MW	$6.4 \times (P_n/4000)^{0.67}$
225	Plasma fueling system	27.9		1610 MW	$51.3 \times (P_f/4000)^{0.67}$
226	Other plant equipments	31.6		1610 MW	$58.2 \times (P_f/4000)^{0.67}$
228	Instrumentation and control	16.9		1610 MW	$31.1 \times (P_f/4000)^{0.67}$
23	Turbine plant equipment	82.2		244 MW	$332.5 \times (P_{th}/1400)^{0.8}$
24	Electrical equipment	143.2		1052 MW	$161.2 \times (P_e/1400)^{0.4}$
25	Miscellaneous plant equipment	59.6		1000 MW	$69.2 \times (P_{net}/1200)^{0.3}$
90	Total direct cost	1007.8			
91–3	Indirect cost	585.6			$0.581 \times (90)$
94	Interest during construction	136.4			$0.0856 \times (90 + 91)$
99	Total plant capital cost	1729.8			

*The following assumptions are made:

interest during construction = 0.0856

plant lifetime = 30 yr

indirect cost factor = 0.581

average load factor = 0.75.

very attractive characteristics compared with D-T fusion power plants is the safety and environmental features. Since the 14-MeV neutron yields are 0.01 to 0.017 times that from an equivalent D-T power plant, the Artemis structure can be disposed of as low-level waste after a full reactor lifetime. Although analyses of the decay heat and tritium release associated with certain accidents need to be researched, the inherent safety of the Artemis power plant is evident because of its small neutron yield and its small tritium exhaust of 8.6 mg/min.

So far we have studied the attractive characteristics

of a D-^{3}He-fueled FRC reactor. The present level of the research on FRCs is, however, rather low, and many issues should be resolved before accepting a D-^{3}He-fueled FRC as a commercial reactor. Experimental verification of the stabilization effects of energetic beam particles on the macroscopic modes in a large-s FRC, which have been indicated by analyses on simple models and numerical simulations, is the most critical issue. An intermediate-scale FRC device, which is able to trap energetic particles, is needed to carry out the experiments and to prove the principles of the fusion plasma. Formation of an FRC with a low filling gas pressure of 0.05 Pa so as to produce a high-T_e initial FRC plasma is also an issue to be studied. Although the filling gas pressure is nearly one order of magnitude lower than that in current experiments, existing small-scale FRC devices can give physics bases relevant to intermediate-scale FRC experiments as well as a commercial reactor. Other physics issues that lie between this study and the final product are the experimental verification of the fluxing of the FRC and controls of the energy transport, a part of which can also be studied with existing small-scale FRC devices.

In the Artemis design, the heating power is supplied by 1-MeV neutral beam particles, which is high compared to the currently available value of 0.3 MeV. Development of a high-energy neutral particle beam is one of the engineering issues in achieving the reactor. The other engineering issue is to complete high-efficiency direct energy converters, which are inevitably needed to realize the favorable characteristics of D-^{3}He fuels in commercial reactors.

VII. SUMMARY OF THE RESULTS

A conceptual design of the D-^{3}He-fueled FRC fusion reactor Artemis was carried out. The FRC is chosen to confine the D-^{3}He burning high-beta plasma since it is surrounded by open field lines suitable for installing high-power direct energy converters to extract most of the fusion energy. By the choice of an FRC, a very compact fusion plasma and a linear reactor geometry, which is convenient for disassembly and repair of the reactor, are gained. This configuration contrasts with that of a D-^{3}He tokamak, where the volume of the plasma is fairly large and most of the fusion energy is carried by radiation.

Energetic beam particles play an important role in the Artemis design. These beam particles stabilize the FRC plasma from tilt modes as well as rotational modes. Furthermore, they drive the plasma current needed to develop and sustain the plasma in a steady burning equilibrium. In a D-^{3}He FRC reactor, the energetic beam particles are supplied by NBI during the preignition phase and by preferential trapping of fusion protons in the FRC during the steady burning phase. Thus, the D-^{3}He FRC appears to be attractive with respect to stability as well as the sustainment of a steady equilibrium. The stabilization effect attributed to energetic beam particles is one of the most important areas to be examined in experiments.

The concept of a traveling wave direct energy converter was developed to extract the fusion energy carried by 14.7-MeV fusion protons. The technologies needed for this development are conventional. The lifetimes of existing structural ferritic steels are as long as the total reactor life of the Artemis, and no development of new materials is necessary. Fuel injection is simple with the moving FRC method. Operation of large and extremely high field magnetic coils is not required. Thus, the bases of technologies employed for Artemis design are conventional and have great technological flexibility that enables the design to accommodate large varieties of unknown parameters.

The estimated COE from Artemis is ~30 mill/kW·h, which is low compared with an LWR or a tokamak reactor. The COE depends only weakly on the fuel cost. Low radioactivity, low tritium yields, and the inherent safety of the power plant may be socially and ecologically acceptable.

Although studies on issues such as stabilization of macroscopic modes by means of energetic particles should be carried out, the characteristics of a D-^{3}He-fueled FRC fusion power plant offer the most attractive prospect for energy development for the 21st century.

ACKNOWLEDGMENTS

This work is supported by a grant-in-aid for fusion research from the Japanese Ministry of Education, Science, and Culture, by a cooperative program of the National Institute for Fusion Science, and by the Lunar Base and Lunar Resources Associate program organized by the Institute for Future Technology and the U.S. Department of Energy.

REFERENCES

1. G. L. KULCINSKI, "Radiation Damage by Neutrons to Materials in DT Fusion Reactors," *Proc. 5th Int. Conf. Plasma Physics and Controlled Fusion Research*, Tokyo, Japan, November 11–15, 1974, Vol. 2, p. 251, International Atomic Energy Agency (1975).

2. R. W. CONN, "First Wall and Divertor Plate Material Selection in Fusion Reactors," *J. Nucl. Mater.*, **76 & 77**, 103 (1978).

3. H. MOMOTA et al., "D^{3}He Fuels in a Field-Reversed Configuration," *Nucl. Instrum. Methods*, **A271**, 7 (1988).

4. W. KERNBICHLER and M. HEINDLER, "Neutron-Lean Fusion Reactor Studies for Thermal Plasmas," *Nucl. Instrum. Methods*, **A271**, 65 (1988).

5. R. E. SIEMON et al., "Review of the Los Alamos FRX-C Experiment," *Fusion Technol.*, **9**, 13 (1986).

6. M. TUSZEWSKI, "Field Reversed Configurations," *Nucl. Fusion*, **28**, 2033 (1988).

7. G. H. MILEY et al., "Preliminary Design of a Self-Sustained Advanced-Fuel Field Reversed Mirror Reactor—SAFFIRE," *Trans. Am. Nucl. Soc.*, **30**, 47 (1978).

8. W. KERNBICHLER et al., "D-^{3}He in Field-Reversed Configurations—RUBY, An International Reactor Study," *Proc. 13th Int. Conf. Plasma Physics and Controlled Nuclear Fusion Research*, Washington, D.C., October 1–6, 1990, IAEA-CN-53/G-2-3, International Atomic Energy Agency (1990).

9. L. C. STEINHAUER and A. ISHIDA, "Gyroviscous Stability Theory with Application to the Internal Tilt Mode of a Field-Reversed Configuration," *Phys. Fluids*, **B2**, 2422 (1990).

10. C. MEHANIAN and R. D. LOVELACE, "Spheromak Tilt Stabilization with an Energetic Particle Component," *Phys. Fluids*, **31**, 1681 (1988).

11. Y. NOMURA, "Suppression of Tilting Instability of a Compact Torus by Energetic Particle Beams," *J. Phys. Soc. Jpn.*, **54**, 1369 (1985).

12. D. C. BARNES and R. D. MILROY, "Stabilization of the Field-Reversed Configuration (FRC) Tilt Instability with Energetic Ion Beams," *Phys. Fluids*, **B3**, 2609 (1991).

13. G. L. KULCINSKI et al., "APOLLO—An Advanced Fuel Fusion Power Reactor for the 21st Century," *Fusion Technol.*, **15**, 1233 (1989).

14. H. L. BERK et al., "Plasma Current Sustained by Fusion Charged Particles in a Field-Reversed Configuration," *Phys. Fluids*, **30**, 3548 (1987).

15. S. P. AUERBACH and W. C. CONDIT, "Classical Diffusion in a Field-Reversed Mirror," *Nucl. Fusion*, **21**, 927 (1981).

16. H. MOMOTA et al., "Feasibility of Poloidal Superconducting Coils for a Medium Size Tokamak," *Proc. 13th Symp. Fusion Technology*, Varese, Italy, September 24–28, 1984, Vol. 2, p. 1463 (1984).

17. R. W. MOIR and W. L. BARR, "Venetian-Blind Direct Energy Converter for Fusion Reactors," *Nucl. Fusion*, **13**, 35 (1973).

18. H. MOMOTA, "Direct Energy Conversion of 15 MeV Fusion Protons," LA-11808-C, p. 8, Los Alamos National Laboratory (1989).

19. D. W. FRY et al., "Travelling-Wave Linear Accelerator for Electrons," *Nature*, **160**, 351 (1947).

20. B. G. LOGAN et al., "Summary of the United States Senior Committee on Environmental, Safety, and Economic Aspects of Magnetic Fusion Energy (ESECOM)," *Proc. 12th Int. Conf. Plasma Physics and Controlled Fusion Research*, Nice, France, October 12–19, 1988, Vol. 3, p. 325, International Atomic Energy Agency (1989).

21. L. J. WITTENBERG et al., "Lunar Source of ^{3}He for Commercial Fusion Power," *Fusion Technol.*, **10**, 167 (1986).

22. J. P. HOLDREN et al., "Summary of the Report of the Senior Committee on Environmental, Safety, and Economic Aspects of Magnetic Fusion Energy," UCRL-53766-Summary, Lawrence Livermore National Laboratory (1987).

23. H. MOMOTA et al., under preparation for publication; see also LA-11808-C, pp. 44 and 49, Los Alamos National Laboratory (1989).

24. M. OHNISHI et al., "Suppression, by Ion Beams, of the $m = 2$ Rotational Instability in a Field Reversed Configuration," *Nucl. Fusion*, **28**, 1427 (1988).

25. Y. OHARA et al., "A Review of JAERI R&D Activities on the Negative-Ion-Based Neutral Beam Injection System," JAERI-M 90-154, Japan Atomic Energy Research Institute (1990).